

# Numerical simulation for mechanism of material surface hardening by high energy electron beam in atmosphere

DENG Yong-feng<sup>1</sup>, LIN Rong<sup>1</sup>, HAN Xian-wei<sup>1</sup>, TAN Chang<sup>1</sup>,  
R. N. Rizakhanov<sup>2</sup>, A. A. Barmin<sup>2</sup>

(1. Shaanxi Power Machine Design and Research Institute, Xi'an 710100, China;  
2. Keldysh Research Center, Moscow 125438, Russia)

**Abstract:** A robust multi-stage numerical model is established to analyze the interaction process and phase-structure transform which occurs in the material surface layer during the material surface hardening by means of electron beam. By the model, it gives a calculation ability of the model to deal with the multi-parameter problem arising from electron beam transportation, temperature evolution and phase transform dynamics. The relationship between the input parameters and formation of structure-phase is obtained.

**Keywords:** material hardening; electron beam; numerical model

**CLC number:** TB3 **Document code:** A **Article ID:** 1672-9374 (2011) 02-0060-07

## 0 Introduction

The research field of material surface modification by using high energy electron beam attracts much attention<sup>[1-4]</sup>. The beam energy can be transformed into the heat of material surface layer in very short time, thus the material surface layer temperature changes quickly, which leads to a great gradient of material temperature<sup>[5-6]</sup>. Consequently the material phase and micro-structure in such layer changes. This transform would always improve the material characteristics. However, the traditional technique of the modification by electron beam is carried out in vacuum<sup>[7]</sup>. Thereby, the efficiency is greatly limited and the modification cost is considerably increased.

In order to resolve the problem, a innovational technique using electron beam in atmosphere is proposed. With this technique, the high energy electron beam is transported into atmosphere through a multi-level differential pumping section<sup>[8-9]</sup>. Therefore, the vacuum technique is unnecessary for material modification, one can use the beam to harden the material in atmosphere directly, and the modification efficiency can be greatly improved. Note that the process is determined by several factors, such as beam energy, beam current and surface structures. Thus it makes the process become even complicated. In this work, a multi-stage numerical model including processes of beam heating and phase transformation is established to investigate the mechanism of material modification process.

收稿日期: 2010-12-13; 修回日期: 2011-01-25

基金项目: 国家自然科学基金项目(No.10905044, No.50911120076)

作者简介: 邓永锋 (1983—), 男, 硕士, 研究领域为等离子体技术

## 1 Numerical model

### 1.1 Physical mechanism

The process of material surface modification by using electron beam can be divided into four stages. First stage defines that the transportation behavior of the beam in atmospheric air until it arrives at material surface. In this process, the characteristics of the beam are determined by gas pressure, gas component and magnetic field. The properties of electron beam are distinct from those of vacuum. Thus, the influences of air scattering should be considered in the model.

Second stage denotes interaction process, which describes the interaction between the beam and material. When the beam arrives at material surface, the beam electrons collide with the material atoms and the energy of electrons is transformed into other forms. One part of the beam energy is transformed into heat of material and the other part of energy is dissipated in environment in the form of scattered electrons and X ray. Aiming at material surface modification, the research of this work focuses on the former part of energy. Usually, this part of energy behaves as the heat source and leads to a sharp increase of material surface layer temperature. In this stage, the model describes the process and then gives the heat source function, which would be used in next simulation stage.

Third stage focuses on the evolution of temperature field by considering the surface state. As mentioned in the second stage, the heat source leads to the increase of temperature. Note that the evolution of material temperature field determines the material metallographic structures. Thereby a two dimensional heat transfer sub-module is included in the model in order to obtain the temperature characteristics.

The fourth stage describes the changes of microstructures and phase transform.

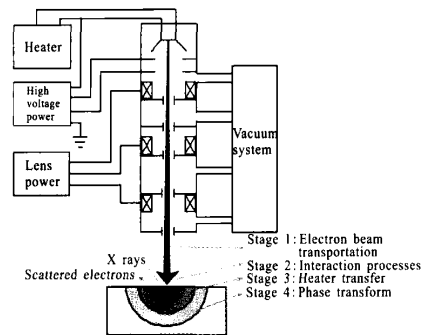


Fig. 1 Schematic diagram of material surface hardened by electron beam in atmosphere

### 1.2 Model of heat source

One should consider the difference between the primary electrons and the local particles if the electron beam is used to harden materials under the condition of atmospheric pressure. It is due to the electron beam always changes its angle, radial distribution and energy spectrum on the way of propagation. When the beam reaches the material surface, it penetrates into the material and loses energy in local region during collisions. The size of this region is determined by two parameters, i.e. beam penetration depth and radial size. By analyzing the process, the penetration depth equals the range of the beam in material, whereas the radial size is determined by property of material surface and distribution of electron beam. Finally, the region can be treated as the dense volume heat source. This process is considered in the first and second stages of the numerical model. Therefore, the following key factors should be included:

- 1) The energy distribution in different medium, i.e. initial cross section of electron beam, the multi-level differential pumping section and gas medium;
- 2) The magnetic field which is used to confine the beam;
- 3) The energy deposition of electrons in gas and material;

4) The reflection of electrons by materials.

Furthermore, when the numerical model is established, the following parameters and characteristics should be taken into account:

-The size and shape of material sample, the initial radial and longitudinal distribution of electron beam.

-The energy spectrum of the beam.

-The chemical components of gas and material, pressure and temperature of gas medium.

-The distribution of magnetic field in multi-level differential pumping section.

-The physical process occurs when electron beam propagates in material.

In order to select a suitable Monte Carlo software which can be used to achieve the micro particles trajectory in material, lots of available Monte Carlo softwares are analyzed and discussed. Finally, GEANT4 (Geometry and Tracking) seems to be a suitable one, which is developed by an international collaboration<sup>[10-11]</sup>. GEANT4 is a free software package written in C++ which can be used to accurately simulate the passage of particles through matter. Now it is widely used in high energy physics, space science and medical fields. When the user comes to his concrete application, he needs to construct the detector geometry, specify the physics list and generate a primary event. Moreover, in order to extract the information he is interested in, the user is asked to construct other GEANT4 user-action modules.

With GEANT4, the trajectory of electron beam and the energy deposition of high energy electron were obtained and analyzed by the aid of a so-called data analysis software AIDA, which is a standard data analysis tool and is widely used in particle physics.

### 1.3 Evolution of surface temperature

The evolution of surface temperature is described by Eq.(1) and is resolved in the third stage by considering heat flux function of structure and phase. The primary problem is three dimension. Moreover,

the spatial and temporal variation of the heat source and the complex shape of material sample make the problem even more complicated, and only can be solved by numerical method.

$$c(T)\rho(T)\frac{\partial T}{\partial t} = \nabla \cdot [\lambda(T)\nabla T] + Q_{eb}(T) + Q_{ph}(T) \quad (1)$$

Where  $c(T)$  is specific thermal capacity,  $\rho(T)$  is density,  $\lambda(T)$  is thermal conduction coefficient,  $T$  is function of temperature,  $Q_{eb}(T)$  is heat flux of inputting material sample,  $Q_{ph}(T)$  is heat flux during diffusion and phase change.

In the process of establishing the model, the evolution properties of temperature should be considered:

1) The heat source is a temporal and spatial varying volume source.

2) The thermal physics and structure-phase changes only occurs in near surface layer.

3) The material sample is always the part of a product, so it has the final size and complex shape.

4) The physical problems, i.e. the thermal problem and structure-phase problem, are coupled by structure-phase dynamics heat flux function.

When coming to the calculation, a high speed and large memory computer is necessary because of the multi-parameter characteristics of this problem. Hence a parallel numerical method needs to be developed. Fortunately, a sophisticated software named OpenFOAM is adopted to solve the problem. The kernel of OpenFOAM provides several modules, such as initial condition module, boundary condition module and discrete equation module. In OpenFOAM, the differential equations are solved by using the finite volume method and the nonstructural grid. It releases researchers from writing codes and makes them put their attention on the physical problems.

### 1.4 Model of steel structure-phase dynamics

When the electron beam penetrates into the material surface, its kinetic energy transforms into the

heat on material sample. Thus, the phase and structure of near surface layer material change quickly, leading to a so-called self-quenching. So, the material surface (usually martensite) always has the high rigidity. The formation of martensite is determined by two factors: cooling rate and carbon content.

The phase changing process of sub-eutectoid steel can be described as following: firstly, the free ferrite transforms into the high temperature austenite in the region of pearlite; secondly, the lamellar cementite is decomposed in order to guarantee desired amount of free carbon; thirdly, austenite becomes uniform due to the infiltration of carbon.

The beginning and ending point of austenitic transformation temperature usually shifts about 100 K in high heating rate, e.g.  $10^3$  K/s. It greatly reduces the temperature threshold of diffusion process. Hence, the phase changing process described above may occur simultaneously. In the model, these processes should be included so as to make the model even more accurate. It means that both two processes, either decrease of cementite or increase of austenite, should be considered in the numerical model. In the third stage, the phase transform dynamics of material in each grid is determined by heating and cooling processes. For a solid medium, the material properties of each point in the simulation region are assumed as an average value of characteristic volume or crystal grain. The symbols are described as follows.  $f_\gamma, f_p, f_{carb}, f_\alpha$  are the percentage of austenite, pearlite, cementite and ferrite respectively. Moreover, the carbon contents of these phases are also defined. In austenite and cementite, the carbon content is defined as  $\langle C \rangle$  and  $\langle C \rangle_{cem}$  respectively. In ferrite, the carbon content is  $\langle C \rangle_f = \text{const} \approx 0$ . Similarly, in pearlite the carbon content  $\langle C \rangle_p$  is constant and equal to the percentage of mass.

For the lamellar ferrite-pearlite structural sub-eutectoid steel, four parameters are defined.

$\langle C \rangle_0$  is the average content of carbon in the steel.  $\langle C \rangle_{0,cem}$  is the initial content of carbon in the cementite.  $R_g$  is defined as average size or effective radius of crystal grain.  $d_p$  is the average distance between two pearlite layers. Other parameters can be obtained by carbon mass conservation equation.

The thickness of cementite in pearlite is given by  $d_{cem} = \frac{\langle C \rangle_p}{\langle C \rangle_{0,cem} - \langle C \rangle_p}$ . The effective radius of pearlite region is  $R_p = R_g \sqrt{\frac{\langle C \rangle_0}{\langle C \rangle_p}}$ . The initial phase of material has some characteristic properties and also is considered in the model. The percentage of pearlite in the alloy obeys the relation  $f_p = f_{0,cem} + f_{10,\alpha}$ , where  $f_{10,\alpha}$  denotes the relative content of eutectoid ferrite in alloy. The relative content of sub-eutectoid ferrite obeys  $f_{0,p} = 1 - f_{10,\alpha}$ . Thus, the total content of ferrite is  $f_v = f_{10,\alpha} + f_{20,\alpha}$ . The relative content of carbon in cementite is  $f_{0,cem} = \langle C \rangle_0 / \langle C \rangle_{0,cem}$ .

If the heating temperature is higher than  $A_{c1}$ , cementite ( $Fe_3C$ ) is decomposed into free state carbon and ferrite, so that the carbon content of cementite decreases. The carbon content is obtained by Eq. (2).

$$\frac{dC_{cem}}{dt} = \frac{\langle C \rangle_{0,cem}}{t} \exp(-t/t) \tag{2}$$

Where  $t = \frac{\exp(U/RT)}{n_0}$  is the characteristic time of decomposing process of  $Fe_3C$ ,  $U$  is the energy threshold. Based on the temperature dynamics mechanism of crystal grain, the increment of austenite between two sheets is given as:

$$\frac{df_\gamma}{dt} = \frac{D(C,T)}{R_p \alpha_0} \left[ -\exp\left(\frac{L_{\alpha \rightarrow \gamma}(T - A_{c1})}{RTA_{c1}}\right) \right] \tag{3}$$

Where  $\alpha_0$  is the iron crystal parameters,  $L_{\alpha \rightarrow \gamma}$  is the latent heat of  $\alpha \rightarrow \gamma$  process. The diffusion coefficient of carbon is given as:

$$D(C,T) = A(\Theta) \exp(-B(\Theta)) \tag{4}$$

where  $\Theta = (T - T_0) / (T_m - T_0)$ .

In high temperature, the material phase may transform into martensite. It means that the remnant part of ferrite transforms into austenite. Thus, when temperature reaches the transform point  $A_{c3}$  of ferrite-austenite, all crystal grains change into austenite except the remnant carbide:

$$\begin{aligned} f_\gamma &= 1 - f_{0, \text{cem}}, & \text{if } C_{\text{cem}} < C_{0, \text{cem}}, \\ f_\gamma &= 1, & \text{if } C_{\text{cem}} < C_{0, \text{cem}}. \end{aligned} \quad (5)$$

In the austenite, the content of carbon is described by the non-steady diffusion equation as Eq. (6).

$$\frac{\partial C(r, t)}{\partial t} = \frac{\partial}{\partial r} D(C, T) \frac{\partial C(r, t)}{\partial r} \quad (6)$$

where  $0 \leq r \leq \frac{d_{\text{cem}} + d_p}{2}$ . This equation needs to be solved based on the time varying initial condition, which also includes the source function of free carbon in cementite region. If the equation is known at time  $t_0$ , the initial condition for subsequent calculation is given as:

$$\begin{aligned} C^{(0)}(r, t_0) &= C(r, t_0) + \int_0^t \frac{dC_{\text{cem}}}{dt} d\tau, & 0 \leq r \leq \frac{d_{\text{cem}}}{2} \\ C^{(0)}(r, t_0) &= 0, & \frac{d_{\text{cem}}}{2} \leq r \leq \frac{d_{\text{cem}} + h_\gamma}{2} \end{aligned} \quad (7)$$

where  $h_\gamma = d_p f_\gamma / (f_{0,p} - f_{0, \text{cem}})$  is the thickness of austenite. If eutectoid ferrite has already transformed into austenite,  $h_\gamma = d_p$ . When cementite completes the decomposition,  $f_\gamma$  sharply increases to  $f_\gamma + f_{0, \text{cem}}$ . And if pearlite transforms into austenite, the maximum value  $f_{0,p}$  can be obtained. Eq. (6) and (7) are self-consistent because of symmetrical characteristics of lamellar cementite and carbon conservation equation of pearlite region.

The process of pearlite decomposition accompanies that lamellar cementite is transformed into spherical cementite. A smaller spherical cementite, whose radius defines as  $R_p$ , is formed in the center of

spherical steel crystal grain (radius is  $R_g$ ). The carbon which is surrounded by dense non-carbon layer is uniform. The processes described by Eq. (2) and (3) are independent with each other. Therefore, the finish criterion of this stage is a time while cementite is completely decomposed, or all eutectoid ferrite transforms into austenite.

After the decomposition of pearlite, the augment and carbon diffusion in austenite occurs subsequently in the steel crystal grain. The equations of this process are similar with Eq. (2) and (3), but it needs to be modified by considering the spherical symmetrical characteristics of crystal grain.

$$\frac{df_\gamma}{dt} = \frac{D(C, T) f_\gamma^{2/3}}{R_{gr}, \alpha_0} \left\{ 1 - \exp\left(\frac{-L_{\alpha \rightarrow \gamma} (T - A_{c1})}{RTA_{c1}}\right) \right\} \quad (8)$$

$$\frac{\partial C(r, t)}{\partial t} = \frac{1}{r^2} \frac{\partial}{\partial r} r^2 D(C, T) \frac{\partial C(r, t)}{\partial r}, 0 \leq r \leq R_i \equiv R_{gr}(f_\gamma)^{1/3} \quad (9)$$

The initial conditions of Eq. (8) and (9) include two equations, i.e. the carbon conservation equation and another equation which is similar with the sphere symmetrical equation.

In a single steel crystal grain, the diffusion-phase dynamic transform equation and heat transfer equation are coupled by latent heat source equation.

$$Q_{\text{ph}} = -\rho \left( L_{\text{cem}} \frac{f_{0, \text{cem}}}{C} \frac{dC_{\text{cem}}}{dt} + L_{\alpha \rightarrow \gamma} \frac{df_\gamma}{dt} \right) \quad (10)$$

where  $L_{\text{cem}}$  and  $L_{\alpha \rightarrow \gamma}$  are the latent heat in the processes of cementite decomposition and austenite transform respectively.

## 2 Validation of model

The main purpose of this paper is to establish a robust numerical model, which can be used to simulate the material hardening process in which the electron beam is emitted in atmosphere. Therefore, here it just gives some figures obtained in different stages

to validate the model ( see Fig. 2, 3 and 4). A detailed research results are available in other paper.

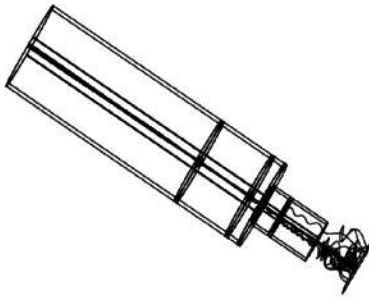
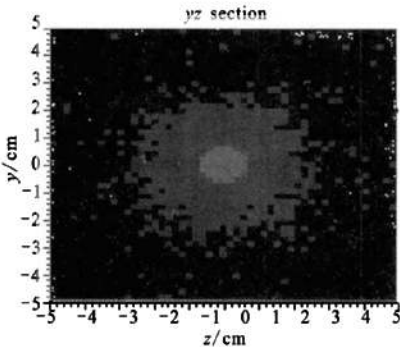
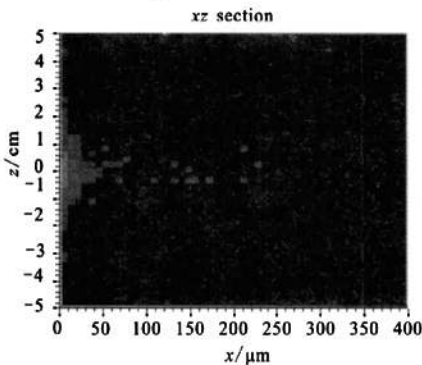


Fig. 2 Electron trajectory during material hardening

The result shown in Fig. 2 was obtained from GEANT4 model in the first stage. It indicates that the beam electrons are scattered by air atoms, which is different from vacuum case. Fig. 3 is the result of energy dissipation distribution in material surface layer. It is given by the model in the second stage.



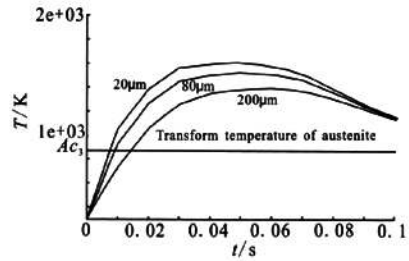
(a) YZ cross section



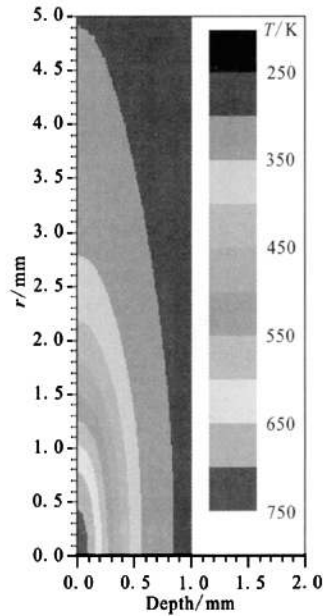
(b) XZ cross section

Fig. 3 Distribution of electron beam energy in the material surface

Fig. 4 gives the evolution of temperature during material hardening. It indicates that the temperature of material reaches the transform point of austenite leading to the transform of micro-structures.



(a) Evolution of temperature during austenite transform



(b) Distribution of temperature

Fig. 4 Evolution of temperature during martial hardening

By analysis, all of the figures indicate that the multi-stage model can be used to investigate the mechanism of material hardening and is so robust that can solve the multi-parameter problem accurately.

### 3 Conclusions

A robust multi-stage numerical model is established to analyze the interaction process, phase-struc-

ture transform which occurs in material surface layer during material hardening by electron beam. By the model, the transportation of high energy electron beam in atmosphere, the interaction between electron beam and material, temperature evolution in material surface layer and phase transform dynamics can be simulated. The calculation ability is achieved to deal with the multi-parameter problem by the model. Therefore, the relationship between the input parameters and formation of structure-phase is obtained.

#### References:

- [1] 王亚军. 电子束加工技术的现状与发展[J]. 航空制造技术, 1995, S1: 28-31.
- [2] 宋红文, 吴伟. 特种加工在航天制造业中应用研究[J]. 机械设计与制造, 2009, 2: 266-268.
- [3] 黄春峰, 赖传兴, 陈树全. 现代特种加工技术的发展[J]. 航空精密制造技术, 2001, 6: 14-20.
- [4] 张紫丽. 发动机研制中的新型表面处理技术[J]. 火箭推进, 1998, 4: 45-51.
- [5] 阎洪. 用电子束进行金属材料表面改性处理[J]. 电加工, 1996, 2: 30-33.
- [6] 秦颖. 强流脉冲电子束材料改性机制及数值模拟[D]. 大连: 大连理工大学, 2004.
- [7] 淡蓝, 七丁. 高能束流加工设备应用调查报告[J]. 航空制造技术, 2009, 9: 72-77.
- [8] HERSHCOVITCH Ady. Air boring and nonvacuum electron beam welding with a plasma window[J]. Physics of Plasmas, 2005, 12 (5): 1-5.
- [9] DENG Yong-feng, HAN Xian-wei, TAN Chang. Monte Carlo simulation of electron beam air plasma characteristics[J]. Chinese Physics B. 2009, 18 (9): 3870-3876.
- [10] AGOSTINELLI S, ALLISON J, MAKO K, et al. GEANT4: a simulation toolkit [J]. Nuclear Instruments and Methods in Physics Research A, 2003, 506: 250-303.
- [11] ALLISON J, MAKO K, APOSTOLAKIS J, et al. Geant4 developments and applications[J]. IEEE Transactions on Nuclear Science, 2006, 53 (1): 270-278.

## 大气环境电子束材料表面强化机理数值模拟

邓永锋<sup>1</sup>, 林榕<sup>1</sup>, 韩先伟<sup>1</sup>, 谭畅<sup>1</sup>, R. N. Rizakhanov<sup>2</sup>, A.A. Barmin<sup>2</sup>

(1.陕西动力机械设计研究所, 陕西 西安 710100; 2.Keldysh Research Center, Moscow 125438, Russia)

**摘要:** 建立了大气环境电子束材料表面强化过程的多阶段数值模型, 用于对电子束与材料表面层的相互作用过程和结构与相变过程进行研究。通过应用这一模型, 使得对材料表面强化中电子束传输、温度演化和相变动力学等多参数研究成为可能, 由此建立了电子束输入参数与结构相变结果之间的关系。

**关键词:** 材料强化; 电子束; 数值模型

**中图分类号:** TB3      **文献标识码:** A      **文章编号:** 1672-9374 (2011) 02-0060-07

(编辑:陈红霞)